CrossMark

RESEARCH PAPER

Development of a simple static microwell array with uniform cell seeding and a chemical concentration gradient

S. I. Yeh[1] · C. C. Hau[1] · C. J. Huang[1] · H. C. Chang[2,3] · C. H. Hsu[3] · J. T. Yang[1]

Abstract For personalized screening and therapeutic inventions across many diseases, the drug–dose response for an individual patient is a major unmet need. In this work, we applied a direct strategy to generate a static microwell array for cell culture with uniform cell seeding and to create the desired chemical concentration gradient into this cell array. It is a simple, novel and easily operable device for a high-throughput drug–dose response experiment that complies with the procedures of cell-based drug screening. Only two repeated operating steps suffice for the entire cell-based drug test—an injection of cells or drug into the flow channel and then injection of air flow into the flow channel. This device comprises two PDMS layers: one side forms an air chamber; the other side forms the liquid channel with embedded cavities as the cells culture and reaction region. The concentration of the drug decreases exponentially along the microwell array; the range of the concentration gradient is varied with the rate of air flow, the volume of the drug plug and the initial concentration of the drug. Small variations of concentration were accessed across varied ranges; the IC_{50} value of DOX in the MDA-MB-231 cell line was thus utilized on this device, precisely and quickly. The IC_{50} value calculated in this work is consistent with the range published elsewhere. With this device, hundreds of data points per compound drug screening can be tested in one experiment, which will be an essential key to determine customized drug dosage and to make possible personalized medicine.

Keywords Static microwell array · Chemical concentration gradient · Cell-based drug testing · IC_{50} value

✉ J. T. Yang
  jtyang@ntu.edu.tw

1 Department of Mechanical Engineering, National Taiwan University, No. 1, Sec. 4, Roosevelt Road, Taipei 10617, Taiwan

2 Program in Tissue Engineering and Regenerative Medicine, National Chung Hsing University, No. 250 Kuo Kuang Road, Taichung 40227, Taiwan

3 Institute of Biomedical Engineering and Nanomedicine, National Health Research Institutes, No. 35 Keyan Road, Miaoli 35053, Taiwan

1 Introduction

Most discussion in personalized medicine, which is a priority of pharmaceutical development, relates to pharmacological therapies (Ginsburg and McCarthy 2001). With the development of personalized medicine, there is tremendous interest, in the pharmaceutical industry, in high-throughput cell-based screening platforms that are capable of rapidly providing precise information on a drug–dose response (Eribol et al. 2016). For personalized screening and therapeutic inventions, the drug–dose response for an individual patient is a major unmet need across many diseases, such as cancer and allergic diseases (Jonas et al. 2015). The most commonly used conventional cell-based systems for drug screening are built on a basis of 96- or 384-well plates and large-scale robotics for liquid handling (e.g., the solution containing cells and a drug at varied concentrations). In the pharmaceutical industry, drug screening is thus a tedious and costly process.

Creating a droplet array or microwell array for a cell culture and generating a concentration gradient in a

🍂 Springer

microfluidic system are the important aspects of biological and medical applications. Droplet-based microfluidics are being widely promoted as a substitute for a conventional well-plate-based screening platform, in which scaling down of the sample size is difficult because of fluid evaporation and pipetting errors (Dressler et al. 2014; Pompano et al. 2011). With droplet-based microfluidics, the droplet arrays fall into two broad categories: a mobile droplet array in which droplets are continuously generated using microfluidic methods (Abate et al. 2010; Ng et al. 2015), and a static microwell array in which the minuscule liquid are stored at predefined locations, to mimic conventional well plates (Bao et al. 2015; Bithi et al. 2014; Hung et al. 2005). The static microwell array is more suitable for drug screening because it allows concurrent and long-term monitoring of several individual microwells in the same field, as in well plates.

Injection with a pipette and a diffusion chamber and diffusion through hydrogels are the most commonly used conventional methods to create a chemical gradient (Kim et al. 2010; Somaweera et al. 2016). Several generators of a concentration gradient in a microfluidic system have been developed. The gradient generators can be classified largely into two groups according to their principle of the generation of a gradient—based on diffusion (Burdick et al. 2004; Kim et al. 2009; Vickerman et al. 2008) and convection (Holden et al. 2003; Huang et al. 2015; Jeon et al. 2000). Most diffusion-based gradient generators lack the dynamic manipulation of a concentration profile; a reservoir of a limited size also affects the gradient stability. In a convection-based gradient generator, streams of fluids composed of varied concentration are brought together in a microfluidic channel in which the solutes are allowed to diffuse across the interface as they flow down the microchannel. The most popular convection-based gradient generator is a microfluidic channel network (Dertinger et al. 2001) because it is flexible in creating and maintaining gradients of varied shapes over long time scales.

With the development of microfluidic technology, especially the droplet array platforms of various types and the established technique of a gradient generator, the rapid, cheap and high-throughput alternatives for drug screening have attracted extensive attention (Dittrich and Manz 2006; Neuži et al. 2012). Microfluidic devices incorporating a gradient generator with multiple cell-culture chambers or droplet arrays are being developed (Chang et al. 2014; Sun et al. 2011; Xu et al. 2013; Yeh et al. 2011; Gao et al. 2012). These devices show a response of the compartmentalized cells to varied concentrations of a drug and serve to determine the pharmacodynamic parameters, such as half-maximal inhibitory concentration (IC_{50} value) of the drug, which is important to ascertain the potency, efficacy and safety of chemotherapeutic agents for individualized drug therapy (Abe et al.

2015; Lee et al. 2015; Toh et al. 2009; Chen et al. 2012). Although several chemical concentration generators have been reported (Kim et al. 2010; Somaweera et al. 2016; Toh et al. 2014; Yang et al. 2015; Xu et al. 2016), the most popular gradient generator is still a microfluidic channel network or its more controllable derivative design, but the range of concentration gradient and the quantity of desired concentration in such a microfluidic channel network are both limited by the complexity of the flow channel.

To accomplish the purpose of cheap and high-throughput drug screening in a simple way, a one-step passive method to create a concentration gradient in a static or mobile well-like array has been reported (Sun et al. 2011; Sun and Vanapalli 2013). This method is capable of generating sequentially a concentration gradient and providing environments of low shear for cell culture, but the reaction regions containing a mixture of cells and drug are sequentially diluted with the buffer with a lack of time for cell growth and differentiation before drug loading in the cell-based drug screening test.

In this work, we present a simple device for a high-throughput drug–dose response experiment that complies with procedures of cell-based drug screening. We use a direct strategy to generate a static microwell array for cell culture with uniform cell seeding and to create a desired gradient of drug concentration in this microwell array. In this chip, the reaction regions and flow channel overlap, which is suitable for cell culture on filling with the culture medium to the upper flow channel. The shear force exerted on the deposited cells by the diluting plug is slight. Only two repeated simple operating steps apply for the entire cell-based drug testing: the injection of cells or drug into a flow channel and then injection of air flow into the flow channel. As an example of cell-based drug screening, the IC_{50} value of DOX in the MDA-MB-231 cell line was derived on the present device. The efficacy of a drug varies significantly among patients because of the variable response to their mechanisms of drug resistance. IC_{50} is the most widely used and informative measure of a drug's efficacy; it indicates how much drug is needed to inhibit a biological process by half, thus providing a measure of potency of an antagonist drug in pharmacological research (Sawant and Shegokar 2014; Saini and Hajrah 2015; Aykul and Martinez-Hackert 2016). The individualized selection of drug doses might bring about the realization of personalized medicine.

2 Experiments

2.1 Device design and fabrication

Figure 1a, b shows the design of this device, which is able to form a static microwell array with uniform cell seeding

and then to generate a chemical concentration gradient in the microwell array. This device, in chip form, comprises two PDMS layers: one side forms an air chamber with the glass substrate; the other side forms the liquid channel (Fig. 1d) with embedded 320 cavities (20×16) as a region for cell culture and cell–drug reaction (Fig. 1e). The PDMS-based membrane between a liquid channel and an air chamber facilitates the generation of a periodic deformation of a membrane that causes a uniform distribution of cells and accelerates the cell–drug interaction in the reaction region (Fig. 1c).

Without a microelectromechanical system (MEMS), common machining processes were utilized to fabricate this device, which includes micromachining with computer numerical control (CNC) to make two molds with microstructures on poly-methylmethacrylate (PMMA) plates, and widely used poly-dimethylsiloxane (PDMS) casting and replication for rapid prototyping of the microfluidic components (Fujii 2002; Eddings and Gale 2006; Lamberti et al. 2014; Yeh et al. 2016). We used two PMMA molds pinching both ends of PDMS to form the main structure with the membrane (thickness 100 μm) therein. The main PDMS structures, plane upper layer (PDMS 1) and glass substrate were bonded together utilizing an oxygen-plasma treatment to form a liquid channel, reaction region and air chamber. The detailed fabrication of this device is shown in supplementary materials, Fig. S1. The width of the liquid channel is 600 μm; the depth is 200 μm. The diameter of the embedded reaction region is 600 μm; the depth is 400 μm. The dimensions of this device are 4.5 cm × 4.5 cm; the volume of each cell culture and cell–drug reaction region is approximately 113 nL.

2.2 Cell and drug preparation

For a cell-based drug screening test, we prepared MDA-MB-231 breast cancer cells (6×10^5 per mL) and doxorubicin (DOX, a chemotherapy drug, Sigma-Aldrich) solution at varied initial concentrations (200, 500 and 1000 μM). The culture medium for MDA-MB-231 cells was supplemented with fetal bovine serum (FBS, 10%). MDA-MB-231 cells were cultured in a standard DMEM medium supplemented with FBS (10%) and penicillin or streptomycin (1%) in a humidified cell incubator (37 °C, CO_2 5%). Before experiments, the cells were cultured to 80% confluence and harvested with trypsin–EDTA. To determine the IC_{50} value, we used Calcein AM (excitation 495 nm, emission 515 nm, Molecular Probes™), which is retained only in live cells, to indicate and to count the number of living cells with a green fluorescent staining.

2.3 Device operation

Figure 2 depicts the operating procedure to generate a static microwell array and to create the concentration gradient. Initially, the culture medium containing cells is injected into the liquid channel (Fig. 2a). Concurrently, the PDMS membrane is deformed periodically with consecutive and periodic air suction. The air suction is provided with a solenoid valve (driving frequency 5 Hz, working pressure as gauge pressure −80 kPa). After the liquid channel is filled with the mixture of the culture medium and cells, we let it stand for 5 min to allow cells to settle to the bottom of the reaction region. An air flow is then injected at a constant flow rate (10 mL/min) to remove superfluous medium and

Fig. 1 **a** Schematic diagram of the chip design. **b** Two chambers of the chip—the liquid chamber and the air chamber. **c** Membranes between two chambers deform periodically to increase the uniformity of cells by periodic air suction. **d** Image of this device, which comprises two inlets, two outlets and a flow channel with embedded cavities. **e** Distribution of 320 (20 × 16) embedded cavities, which are the regions for cell culture and cell–drug reaction of this device. The dimensions of the chip are 4.5 × 4.5 cm²; the volume of each reaction region (the embedded cavity) is 113 nL
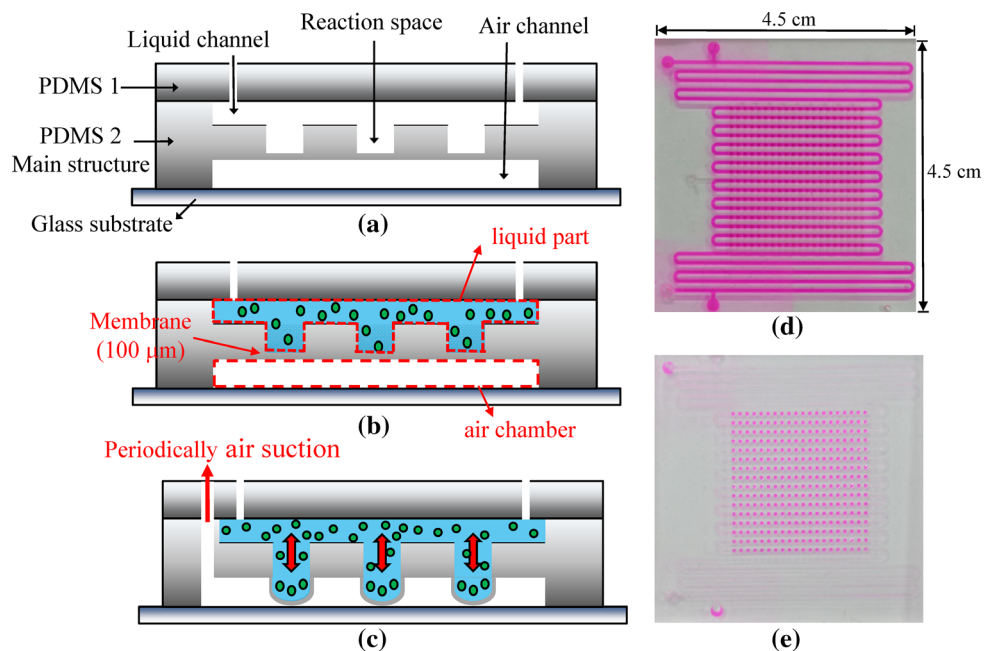
Fig. 2 Schematic illustration of an experimental procedure: **a** inject the cells into the liquid channel and deform the membrane concurrently, **b** inject the air flow to form the static microwell array, **c** inject a drug plug and push it with air, and **d** generate automatically a gradient of drug concentration, **e** analysis steps to determine the IC_{50} value of the specific drug and cell
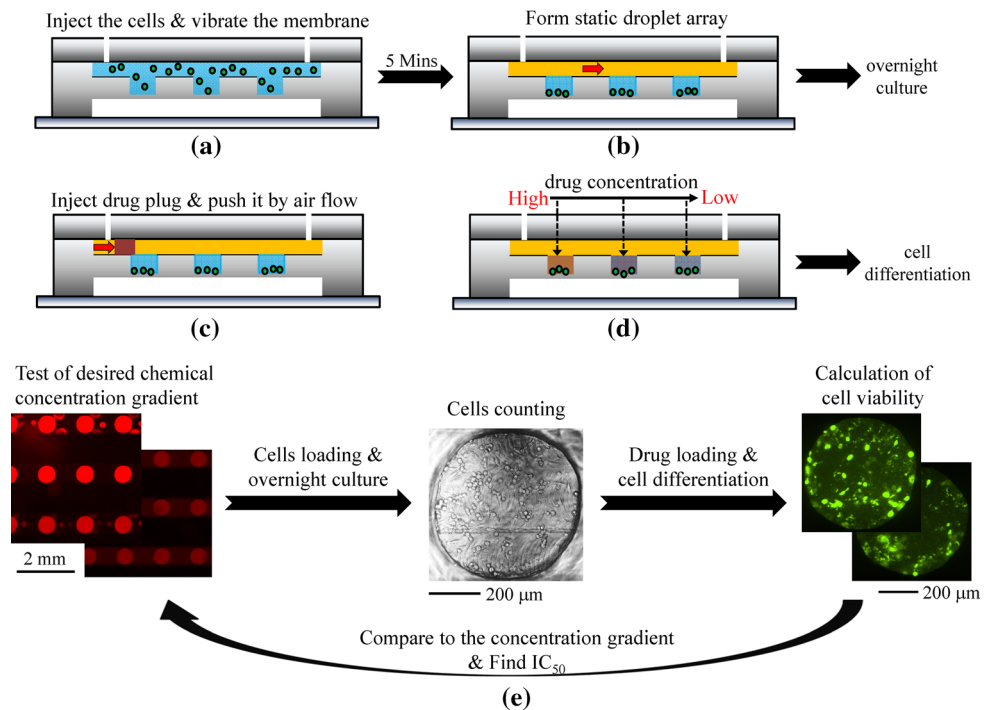
cells outside the reaction region (Fig. 2b) and to form the microwell array. We repeat the cell loading with exchange of inlet and outlet to avoid a decreased number of cells caused by the gravity effect. Then a fresh culture medium (10% FBS) is reloaded into the flow channel every 8 h to provide fresh nutrient in the cell-culture region to keep the cells healthy. This chip is placed in a humidified incubator (CO_2 5%, 37 °C) for overnight culture.

After overnight culture, while the cells are already attached at the bottom of the reaction region, the drug plug is injected into a liquid channel (Fig. 2c). This system exploits the Taylor–Aris dispersion (Taylor 1953) to create a concentration gradient. On pushing the drug plug with an air flow at a constant rate, the drug plug passes through the microwell array sequentially; the drug concentration becomes rapidly and serially diluted in an automatic manner (Fig. 2d). After 48 h for cell differentiation in a humidified incubator (CO_2 5%, 37 °C), we load Calcein AM solution into the flow channel and label the living cells to verify the cell viability in each reaction region.

Figure 2e shows the analysis steps to determine the IC_{50} value of the specific drug and cell line. Initially, we pretested the range of drug concentration gradient and the concentration distribution in each reaction region based on various operating parameters, initial concentrations, rate of air flow and volume of the drug plug. After cell culture, we count the number of cells; we then calculate the cell viability after cell–drug interaction. The IC_{50} value is eventually determined on comparing the distribution of the concentration gradient of the whole array. Because of the consistency

of the distribution of chemical concentration with the same operating parameters, the present device is a useful tool to duplicate the cell-based drug screening test multiple times without preparing or measuring the reagent at varied concentrations.

3 Results and discussion

3.1 Encapsulation of cells in a static microwell array

A poor uniformity of cell number in cell-based drug screening produces an undesirable cellular response and a variable cell–drug interaction. Because of the recirculating flow within the sudden-expansion microchannel or cavity-embedded channel (as Fig. 3a, Iwasa et al. 2003), the cells accumulate in a corner of the reaction region reverse to the flow direction as shown in Fig. 3b. Moreover, the number of cells progressively decreases along the flow direction due to the gravity effect. We inject the cells twice in the reversed flow direction to avoid decreasing the cell number and to create a uniform distribution of cells along this array. A periodic deformation of a PDMS-based membrane utilized in this device is designed to disturb the recirculation flow inside the microwell and to create a uniform distribution of cells inside the microwell.

MDA-MB-231 breast cancer cells (6×10^5 per mL) were loaded into this device and formed a microwell array of encapsulated cells. Figure 3c shows images of the cells that adhered to the bottom of the reaction region in the inlet and

Fig. 3 Uniformity of breast cancer cell MDA-MB-231 (density of injected cells 6×10^5/mL). **a** Schematic illustration of cross section of the flow within a sudden-expansion microchannel or cavity-embedded channel. **b** Without periodic deformation of the membrane, the cells accumulated in a corner of the reaction region reversed to the flow direction. **c** Images of cells at the bottom of reactor near the inlet and outlet regions after periodic deformation of the membrane. **d** Average number of cells in each row of the matrix; the average number of cells is approximately 149 cells per reactor, coefficient of variation (CV) 9.62%
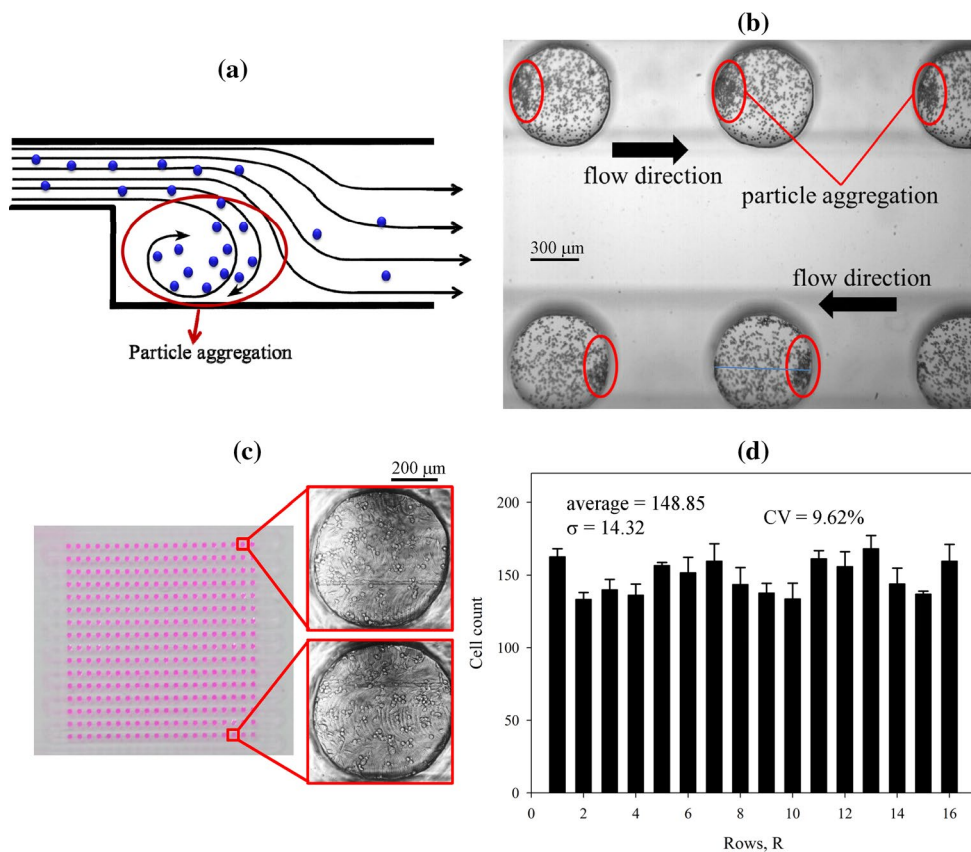
outlet regions after culture overnight. One can see a uniform spatial distribution of cells in each reactor. The cell number, counted (ImageJ, open-source macro, Grishagin 2015) after overnight culture in each row, is shown in Fig. 3d. We used the coefficient of variation, the ratio of the standard deviation to the mean, to represent the uniformity of cells, which is a statistical measure of the dispersion of data points in a data series around the mean. The coefficient of variation in each row is less than 11.6%. For the entire static microwell array, the average number of cells is approximately 149 cells per well; the coefficient of variation is 9.62%. We can see also a uniform spatial distribution over the entire microwell array. Cells of sufficient amount for a drug screening test showed a satisfactory overall uniformity to avoid an undesirable cellular response in drug screening involving cell–cell interaction.

3.2 Generation of a concentration gradient

Figure 4a illustrates that the chemical concentration gradually decreased along the flow direction in the presented device. Figure 4b presents an image of a concentration gradient of a blue dye generated with this device according to the concentration in a descending order shown in Fig. 4a. The DI-water and blue-dye solution served to verify the performance of our serial concentration-generating concept. Water (DI) was first loaded into the channel and formed a static microwell array. A plug (6 μL) containing the blue-dye solution was loaded and pushed to the outlet with an air flow (10 mL/min). The concentration gradient was smoothly generated in the microwell array as the blue-dye solution passed through the reaction region. With the same operating process, a concentration gradient of doxorubicin (DOX) can be generated on the presented device. We measured the fluorescent intensity with varied concentration of DOX with a commercial fluorescence microscope (Nikon A1R). Based on a linear relation between intensity of fluorescence (excitation 488 nm, emission 588 nm) and concentration of DOX (Kawai et al. 1997; Li et al. 2014, also see Fig. S2 in supplementary materials), we quantitated the profile of the DOX concentration gradient along the presented microwell array. Figure 4c shows that the variation of DOX concentration along the flow direction in each microwell (drug plug 6 μL with initial concentration 200 μM pushed with air flow 10 mL/min) fitted an exponential decay function ($R^2 = 0.998$).

Figure 4d–f shows a profile of the concentration gradient along the microwell array on varying the operating parameters; these profiles were measured at the midpoint in each row (red line in Fig. 4b). For all operating conditions, the DOX concentration also decayed exponentially along the flow direction; small variations in concentration
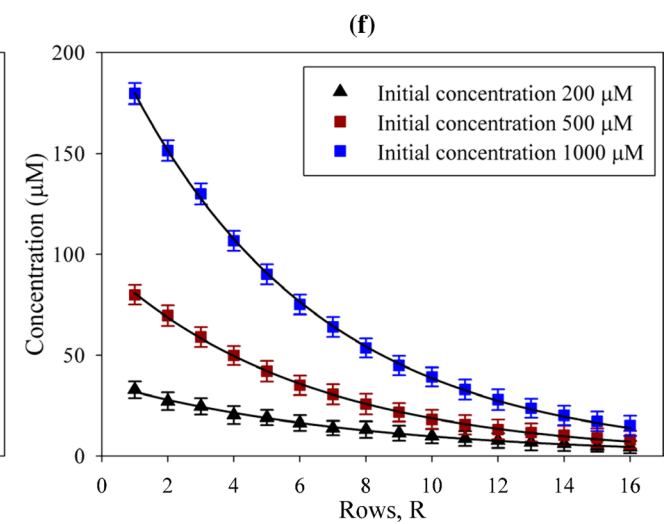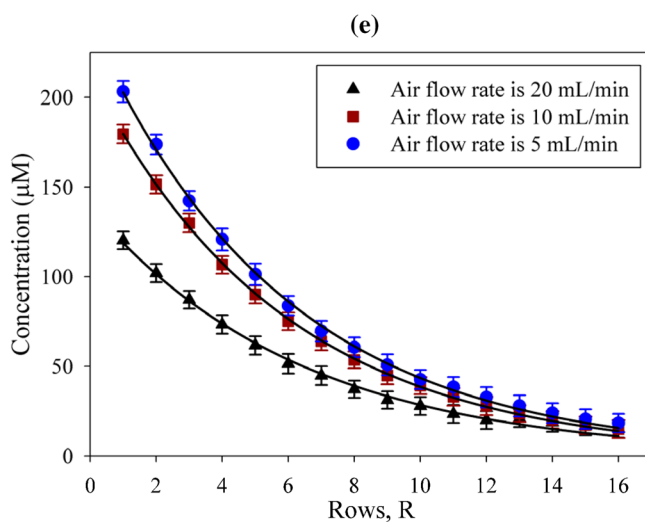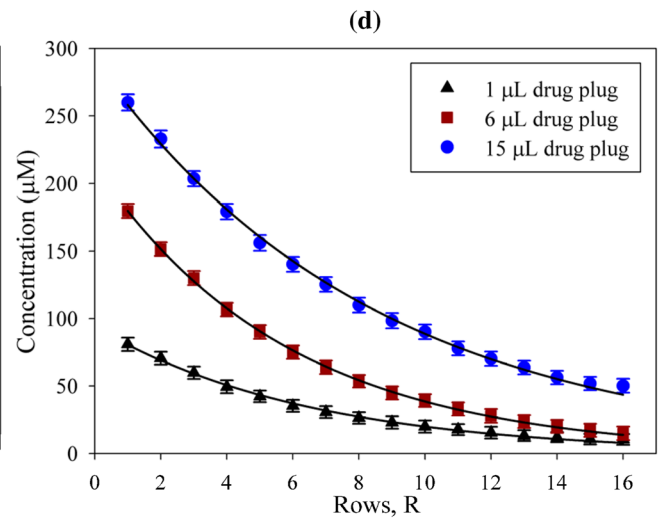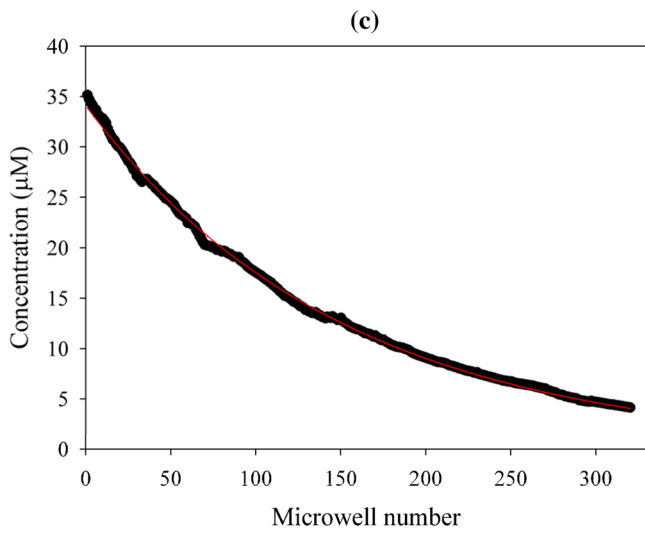
(a)

Inlet

concentration decreased

Outlet

(b)

1 cm

1

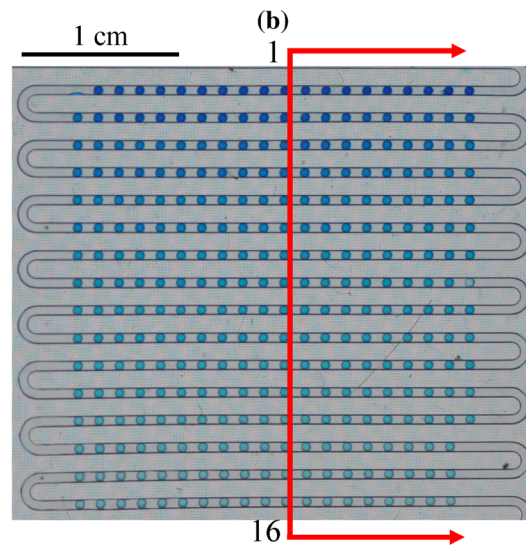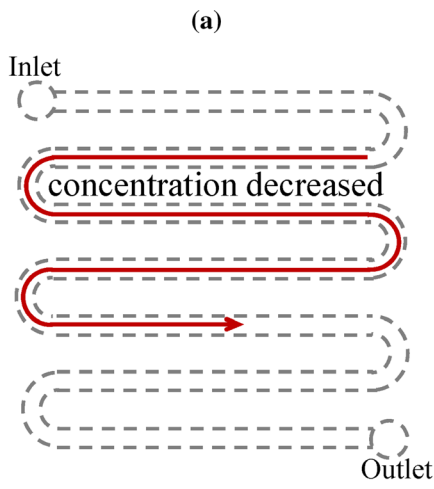16

(c)

(d)

(e)

(f)

◄**Fig. 4** **a** Schematic illustration of chemical concentration gradually decreasing along the flow direction. **b** Concentration gradient of a blue dye generated in a matrix form. **c** Variation of DOX concentration along the flow direction in each microwell (drug plug 6 μL with initial concentration 200 μM pushed with air flow at 10 mL/min). **d**–**f** Control of concentration gradient ranges on varying operating parameters; the concentration of the drug decayed exponentially along the microwell array. **d** With initial concentration 1000 μM, the air flow rate (10 mL/min) was fixed; the volume of drug plug was varied. **e** With initial concentration 1000 μM, the volume (6 μL) of the drug plug was fixed; the air flow rate was varied. **f** The volume of drug plug (6 μL) and the rate (10 mL/min) of air flow were fixed; the range of the concentration gradient was varied with the initial concentrations of drug plug. The concentration gradient profiles were measured at the midpoint in each *row* (*red line*)

were assessed across a range that varied with the rate of air flow, the volume of the drug plug, and the initial concentration of the drug plug. With the same initial concentration (1000 μM) and rate (10 mL/min) of air flow, the larger volume of the drug plug yielded a wider range of concentration gradient and a precipitous change in the gradient (Fig. 4c). In particular, the larger volume of a drug plug caused apparently greater concentrations in the first few rows because of the increased duration for the drug plug to pass through a reaction region (cavity) and the large total drug content in the plug, but a larger volume of the drug plug also caused increased concentrations in the last few rows, which is unsuitable for a low-dose drug.

With the same initial concentration (1000 μM) and volume of drug plug (6 μL), a smaller rate of air flow yielded a wider range of concentration gradient and a precipitous change in gradient because of the increased duration for the drug plug to pass through a reaction region (Fig. 4d). Somewhat differently, the concentrations of the last few rows varied little with the rate of air flow. Furthermore, the varied initial concentrations of the drug plug caused a disparity of concentration in the first few rows, but not in the last few rows (Fig. 4e). The reason is that the larger concentration gradient between the drug plug and the solution in the reaction region increased the mass transfer of drug molecules.

The range of concentration gradient varied with the rate of air flow, the volume of the drug plug and the initial concentration of the drug plug. The maximum range of the concentration gradient in this work was from 50.2 to 259.9 μM with a drug plug (15 μL, 1000 μM) with rate 10 mL/min of air flow. The optimum operating condition depends on the dose range of a specific drug. In this work, referring to other research, DOX (6 μL, initial concentration 200 μM) was injected into the channel and pushed to the outlet with an air flow (10 mL/min) to generate a concentration gradient of DOX from 4.4 to 32.8 μM. On generating small concentration variations of a 320-microwell array automatically, the cell-based drug screening to

determine the precise pharmacodynamic parameters was executed without a cumbersome and costly preparation of a drug.

3.3 Cell-based drug screening test

To test the half-maximal inhibitory concentration (IC_{50} value), MDA-MB-231 cancer cells were first loaded and seeded at the bottom of the microwell array. Chemotherapy drug DOX (6 μL, initial concentration 200 μM) was injected into the channel and pushed to the outlet with air flow 10 mL/min to generate a concentration gradient of DOX with the present strategy. We analyzed the initial concentration gradient of DOX in the microwell array on measuring the fluorescent intensity there. After DOX reacted with cells for 48 h, we labelled the living cells with Calcein AM to verify the cell viability in the midpoint reaction region in each row. As shown in Fig. 5a, green indicates viable cells. The cell viability decreased in an area of large drug concentration (weak fluorescence) and vice versa.

The IC_{50} value of DOX in MDA-MB-231 cell line was calculated in Fig. 5a that shows the cell viability at varied DOX concentration. We ran the cell-based drug screening in five chips; the IC_{50} value calculated in each chip was 6.44, 6.41, 6.38, 6.52 and 6.48 μM. Figure 5b shows the cell viability at varied concentration at the midpoint in each row of the microwell array. The five groups of data points approximately coincide with a profile ($R^2 > 0.99$) of the cell viability at varied DOX concentration. The average IC_{50} value of DOX in MDA-MB-231 cell line was 6.446 ± 0.05 μM, consistent with ranges published elsewhere (Kalet 2007; Tassone et al. 2003; Tegze et al. 2012). The proposed method of measuring IC_{50} through an easily operated microwell array and a concentration-gradient generator shows multiple testing to be highly reliable.

4 Conclusion

In this work, we developed a simple device that contains both a generator of a concentration gradient and a static microwell array. Both the microwell array (with uniform cell seeding) and the gradient were generated with an easy and direct method. The necessary operations are injecting cells, the drug and the air flow in sequence. Hence, this device is quickly and easily operable for cell-based drug screening.

The average number of cells was approximately 149 cells per well; the coefficient of variation was 9.62. We found a uniform spatial distribution in each reactor and over the entire microwell array. A sufficient amount of cells for a drug screening test showed a satisfactory overall uniformity that avoided undesirable cellular responses in drug
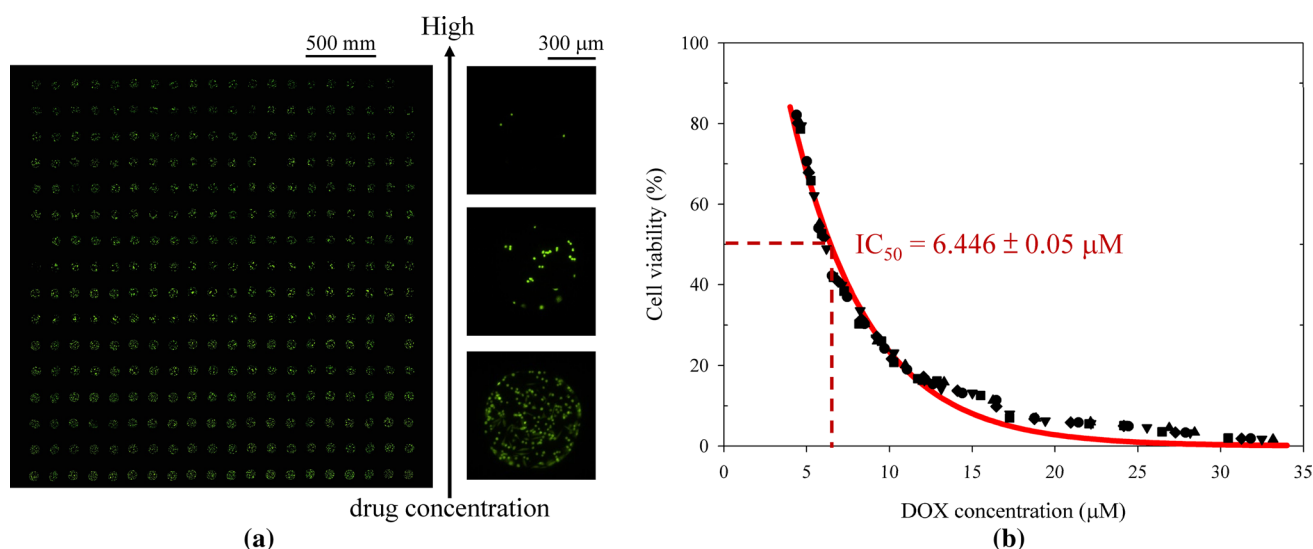
Fig. 5 a Fluorescent intensity test for cells and drug interaction. The cells were labelled with Calcein AM, a membrane-permeable live-cell labelling dye. According to a decreasing drug concentration, the cell viability was gradually enhanced (greater fluorescent response). **b** Multiple testing of cell viability in separate chips. The cell viability of breast cancer cell MDA-MB-231 after treatment with a concentration gradient of DOX for 48 h. The average IC_{50} value is 6.446 ± 0.05 μM. (The *various symbols* represent experimental results conducted in five separate chips)

screening involving cell–cell interactions. Using an optimum operating condition of a DOX plug, the small variations in concentration were accessed from 4.4 to 32.8 μM. Utilizing this device and following the proposed procedure, we found an IC_{50} value of DOX in the MDA-MB-231 cell line consistent with a range reported elsewhere.

This device shows a high potential for a drug-testing application, as demonstrated through easy and precise quantification of the IC_{50} value of DOX in breast cancer cell in vitro. Using this device, hundreds of data points per compound drug screening can be tested in one experiment without cumbersome and costly preparation of a drug. It will be an essential key to determine customized drug dosage and to make possible personalized medicine.

References

Abate AR, Hung T, Mary P, Agresti JJ, Weitz DA (2010) High-throughput injection with microfluidics using picoinjectors. Proc Natl Acad Sci 107(45):19163–19166

Abe Y, Kamiya K, Osaki T, Sasaki H, Kawano R, Miki N, Takeuchi S (2015) Nonlinear concentration gradients regulated by the width of channels for observation of half maximal inhibitory concentration (IC 50) of transporter proteins. Analyst 140(16):5557–5562

Aykul S, Martinez-Hackert E (2016) Determination of half-maximal inhibitory concentration using biosensor-based protein interaction analysis. Anal Biochem 508:97–103

Bao L, Rezk AR, Yeo LY, Zhang X (2015) Highly ordered arrays of femtoliter surface droplets. Small 11(37):4850–4855

Bithi SS, Wang WS, Sun M, Blawzdziewicz J, Vanapalli SA (2014) Coalescing drops in microfluidic parking networks: a multi-functional platform for drop-based microfluidics. Biomicrofluidics 8(3):034118

Burdick JA, Khademhosseini A, Langer R (2004) Fabrication of gradient hydrogels using a microfluidics/photopolymerization process. Langmuir 20(13):5153–5156

Chang CW, Cheng YJ, Tu M, Chen YH, Peng CC, Liao WH, Tung YC (2014) A polydimethylsiloxane–polycarbonate hybrid microfluidic device capable of generating perpendicular chemical and oxygen gradients for cell culture studies. Lab Chip 14(19):3762–3772

Chen CY, Wo AM, Jong DS (2012) A microfluidic concentration generator for dose-response assays on ion channel pharmacology. Lab Chip 12(4):794–801

Dertinger SK, Chiu DT, Jeon NL, Whitesides GM (2001) Generation of gradients having complex shapes using microfluidic networks. Anal Chem 73(6):1240–1246

Dittrich PS, Manz A (2006) Lab-on-a-chip: microfluidics in drug discovery. Nat Rev Drug Discovery 5(3):210–218

Dressler OJ, Maceiczyk RM, Chang S-I (2014) Droplet-based microfluidics enabling impact on drug discovery. J Biomol Screen 19(4):483–496

Eddings MA, Gale BK (2006) A PDMS-based gas permeation pump for on-chip fluid handling in microfluidic devices. J Micromech Microeng 16(11):2396

Eribol P, Uguz A, Ulgen K (2016) Screening applications in drug discovery based on microfluidic technology. Biomicrofluidics 10(1):011502

Fujii T (2002) PDMS-based microfluidic devices for biomedical applications. Microelectron Eng 61:907–914

Gao Y, Sun J, Lin WH, Webb DJ, Li D (2012) A compact microfluidic gradient generator using passive pumping. Microfluid Nanofluid 12(6):887–895

Ginsburg GS, McCarthy JJ (2001) Personalized medicine: revolutionizing drug discovery and patient care. Trends Biotechnol 19(12):491–496

Grishagin IV (2015) Automatic cell counting with ImageJ. Anal Biochem 473:63–65

Holden MA, Kumar S, Castellana ET, Beskok A, Cremer PS (2003) Generating fixed concentration arrays in a microfluidic device. Sens Actuators B: Chem 92(1):199–207

Huang PH, Chan CY, Li P, Nama N, Xie Y, Wei CH, Chen Y, Ahmed D, Huang TJ (2015) A spatiotemporally controllable chemical gradient generator via acoustically oscillating sharp-edge structures. Lab Chip 15(21):4166–4176

Hung PJ, Lee PJ, Sabounchi P, Lin R, Lee LP (2005) Continuous perfusion microfluidic cell culture array for high-throughput cell-based assays. Biotechnol Bioeng 89(1):1–8

Iwasa J, Ochi M, Uchio Y, Katsube K, Adachi N, Kawasaki K (2003) Effects of cell density on proliferation and matrix synthesis of chondrocytes embedded in atelocollagen gel. Artif Organs 27(3):249–255

Jeon NL, Dertinger SK, Chiu DT, Choi IS, Stroock AD, Whitesides GM (2000) Generation of solution and surface gradients using microfluidic systems. Langmuir 16(22):8311–8316

Jonas O, Landry HM, Fuller JE, Santini JT, Baselga J, Tepper RI, Cima MJ, Langer R (2015) An implantable microdevice to perform high-throughput in vivo drug sensitivity testing in tumors. Sci Transl Med 7(284):284ra257

Kalet BT (2007) Doxorubicin and its formaldehyde conjugates (Doctoral dissertation, University of Colorado at Boulder)

Kawai H, Minamiya Y, Kitamura M, Matsuzaki I, Hashimoto M, Suzuki H, Abo S (1997) Direct measurement of doxorubicin concentration in the intact, living single cancer cell during hyperthermia. Cancer 79(2):214–219

Kim D, Lokuta MA, Huttenlocher A, Beebe DJ (2009) Selective and tunable gradient device for cell culture and chemotaxis study. Lab Chip 9(12):1797–1800

Kim S, Kim HJ, Jeon NL (2010) Biological applications of microfluidic gradient devices. Integr Biol 2(11–12):584–603

Lamberti A, Marasso SL, Cocuzza M (2014) PDMS membranes with tunable gas permeability for microfluidic applications. Rsc Adv 4(106):61415–61419

Lee DW, Lee M-Y, Ku B, Nam D-H (2015) Automatic 3d cell analysis in high-throughput microarray using micropillar and microwell chips. J Biomol Screen. doi:10.1177/1087057115597635

Li X, Zhang X, Zhao S, Wang J, Liu G, Du Y (2014) Micro-scaffold array chip for upgrading cell-based high-throughput drug testing to 3D using benchtop equipment. Lab Chip 14(3):471–481

Neuži P, Giselbrecht S, Länge K, Huang TJ, Manz A (2012) Revisiting lab-on-a-chip technology for drug discovery. Nat Rev Drug Discov 11(8):620–632

Ng EX, Miller MA, Jing T, Lauffenburger DA, Chen C-H (2015) Low-volume multiplexed proteolytic activity assay and inhibitor analysis through a pico-injector array. Lab Chip 15(4):1153–1159

Pompano RR, Liu W, Du W, Ismagilov RF (2011) Microfluidics using spatially defined arrays of droplets in one, two, and three dimensions. Annu Rev Anal Chem 4:59–81

Saini KS, Hajrah NH (2015) Toxicogenomics–getting us a step closer towards personalized medicine. J Investig Genomics 2(3):00024

Sawant S, Shegokar R (2014) Cancer research and therapy: where are we today? Int J Cancer Therapy Oncol 2(4):02048

Somaweera H, Ibraguimov A, Pappas D (2016) A review of chemical gradient systems for cell analysis. Anal Chim Acta 907:7–17

Sun M, Vanapalli SA (2013) Generation of chemical concentration gradients in mobile droplet arrays via fragmentation of long immiscible diluting plugs. Anal Chem 85(4):2044–2048

Sun M, Bithi SS, Vanapalli SA (2011) Microfluidic static droplet arrays with tuneable gradients in material composition. Lab Chip 11(23):3949–3952

Tassone P, Tagliaferri P, Perricelli A, Blotta S, Quaresima B, Martelli M, Goel A, Barbieri V, Costanzo F, Boland C (2003) BRCA1 expression modulates chemosensitivity of BRCA1-defective HCC1937 human breast cancer cells. Br J Cancer 88(8):1285–1291

Taylor G (1953) Dispersion of soluble matter in solvent flowing slowly through a tube. In: Proceedings of the royal society of London a: mathematical, physical and engineering sciences. The Royal Society 1137:186–203

Tegze B, Szállási Z, Haltrich I, Pénzváltó Z, Tóth Z, Likó I, Győrffy B (2012) Parallel evolution under chemotherapy pressure in 29 breast cancer cell lines results in dissimilar mechanisms of resistance. PLoS ONE 7(2):e30804

Toh YC, Lim TC, Tai D, Xiao G, van Noort D, Yu H (2009) A microfluidic 3D hepatocyte chip for drug toxicity testing. Lab Chip 9(14):2026–2035

Toh AG, Wang Z, Yang C, Nguyen N-T (2014) Engineering microfluidic concentration gradient generators for biological applications. Microfluid Nanofluid 16(1–2):1–18

Vickerman V, Blundo J, Chung S, Kamm R (2008) Design, fabrication and implementation of a novel multi-parameter control microfluidic platform for three-dimensional cell culture and real-time imaging. Lab Chip 8(9):1468–1477

Xu BY, Hu SW, Qian GS, Xu JJ, Chen HY (2013) A novel microfluidic platform with stable concentration gradient for on chip cell culture and screening assays. Lab Chip 13(18):3714–3720

Xu Z, Huang X, Wang P, Wang H, Weitz DA (2016) Optimization and development of a universal flow-based microfluidic gradient generator. Microfluid Nanofluid 20(6):1–10

Yang CG, Liu YH, Di YQ, Xu ZR (2015) Generation of two-dimensional concentration-gradient droplet arrays on a two-layer chip for screening of protein crystallization conditions. Microfluid Nanofluid 18(3):493–501

Yeh CH, Chen CH, Lin YC (2011) Use of a gradient-generating microfluidic device to rapidly determine a suitable glucose concentration for cell viability test. Microfluid Nanofluid 10(5):1011–1018

Yeh SI, Fang WF, Huang CJ, Wang TM, Yang JT (2016) The visual colorimetric detection of multi-nucleotide polymorphisms on a pneumatic droplet manipulation platform. J Vis Exp 115:e54424–e54424